Journal of Alloys and Compounds 509 (2011) 4060–4064

Contents lists available at ScienceDirect

Journal of Alloys and Compounds

journal homepage: www.elsevier.com/locate/jallcom

Effect of annealing temperature on the structure and optical properties of sputtered TiO_2 films

Baoxing Zhao, Jicheng Zhou*, Yu Chen, Yinqiao Peng

School of Energy Science and Engineering, Central South University, Changsha 410083, China

ARTICLE INFO

Article history:
Received 23 July 2010
Received in revised form
31 December 2010
Accepted 3 January 2011
Available online 5 January 2011

Keywords:
Thin films
Vapor deposition
Microstructure
Optical properties

ABSTRACT

TiO_2 thin films were deposited by DC reactive magnetron sputtering. Some TiO_2 thin films samples were annealed for 5 min at different temperatures from 300 to 900 °C. The structure and optical properties of the films were characterized by X-ray diffraction (XRD), field emission scanning electron microscopy (SEM) and ultraviolet–visible (UV–vis) spectrophotometry, respectively. The influence of the annealing temperature on the structure and optical properties of the films was investigated. The results show that the as-deposited TiO_2 thin films are mixtures of anatase and rutile phases, and possess the column-like crystallite texture. With the annealing temperature increasing, the refractive index and extinction coefficient increase. When the annealing temperature is lower than 900 °C, the anatase phase is the dominant crystalline phase; the weight fraction of the rutile phase does not increase significantly during annealing process. As the annealing temperature rises to 900 °C, the rutile phase with the large extinction coefficient becomes the dominant crystalline phase, and the columnar structure disappears. The films annealed at 300 °C have the best optical properties for the antireflection coatings, whose refractive index and extinction coefficient are 2.42 and 8×10^{-4} (at 550 nm), respectively.

© 2011 Elsevier B.V. All rights reserved.

1. Introduction

Titanium dioxide (TiO_2) thin films have a long history in silicon photovoltaics (PV) as antireflection (AR) coatings [1]. TiO_2 thin films have many advantages, including their very good chemical resistance to the majority of chemicals used in the PV industry and their optimal refractive index for glass encapsulated silicon solar cells [2]. From the three crystalline phases (anatase, rutile, and brookite) in titanium oxides, the anatase phase is desired in AR coatings applications because of its high refraction index and low extinction coefficient [3]. Moreover, the anatase TiO_2 films have numerous interesting applications in optical coatings, optical waveguides, photo-decomposition of environmental pollutants, solar cells and electronic devices [4–6]. Many different procedures for the preparation of TiO_2 thin films are reported [7–10]. Among these deposition methods, the magnetron sputtering is very attractive due to many advantages, such as the freedom to choose substrate material, low deposition temperature and a uniform deposition over a relatively larger area. Unfortunately, the anatase phase is not thermodynamically stable. This instability arises from the transition of anatase to rutile. Therefore, the optimization of the annealing process is important. A large number of studies have reported the transition temperature is about 700 °C [10]. For physical vapour deposition (PVD), the actual temperature range of this transition depends on the details of the preparation conditions. For instance, Ben Amor et al. [11] found that the anatase phase is stable at 800 °C and the anatase completely transforms to the rutile at 1200 °C. Tian et al. [12] reported that annealing at 1100 °C only leads to the growth of the anatase crystallite, and the rutile phase does not appear. Whereas some studies showed that the anatase completely transforms to the rutile phase when annealed at about 900 °C [13]. Hunsche et al. [14] even found that the transition starts at 500 °C. However, few reports try to explain these differences. This research aims to investigate the effect of annealing temperature on the crystalline structure and optical properties of the TiO_2 thin film prepared by DC reactive magnetron sputtering. Furthermore, the relations between thermal stability and microstructure of the sputtered TiO_2 thin films were tried to be established.

2. Experimental

TiO_2 thin films were deposited at room temperature by DC reactive magnetron sputtering of a Ti target (purity 99.99% and diameter 100 mm). The oxygen (O_2) and argon (Ar) were used as reactive gas and working gas, respectively. The sputtering pressure was kept at 0.7 Pa, with an O_2 flow rate of 10 mL/min and an Ar flow rate of 90 mL/min. A turbo molecular pump was used to achieve a base pressure of 1×10^{-3} Pa. The target-to-substrate distance was kept constant at 60 mm. The sputtering power was kept at approximately 400 W. Quartz glass plates with size of 25 mm × 25 mm × 1 mm were used as substrates. The substrates were ultrasonically cleaned in acetone, ethyl ethanol and deionized water for 15 min in sequence, then dried by N_2. The pre-sputtering was performed for 5 min to clean the surface of the

* Corresponding author. Tel.: +86 13873193957.
E-mail address: jicheng@mail.csu.edu.cn (J. Zhou).

0925-8388/$ – see front matter © 2011 Elsevier B.V. All rights reserved.
doi:10.1016/j.jallcom.2011.01.020

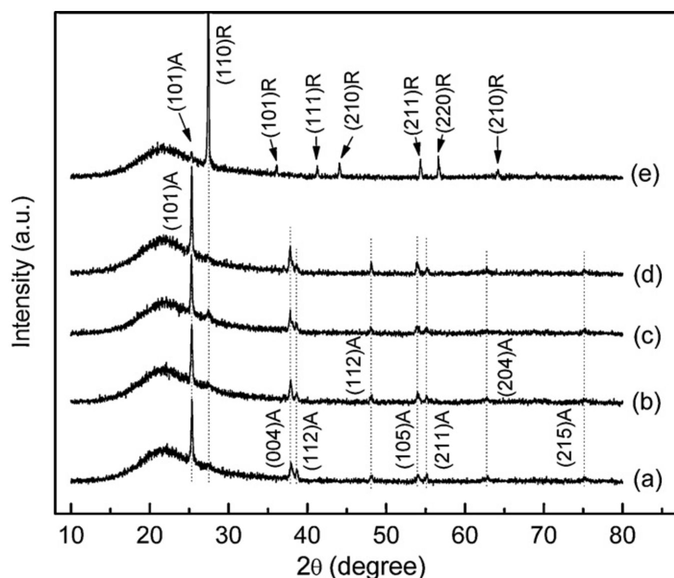

Fig. 1. XRD patterns for the TiO_2 films annealed at different temperatures: (a) as-deposited; (b) 300 °C; (c) 500 °C; (d) 700 °C; (e) 900 °C.

titanium target, and then the TiO_2 thin films were deposited at room temperature for 50 min. For the annealing studies, some samples were annealed by RTP-500 rapid thermal processor at 300, 500, 700 and 900 °C for 5 min, respectively.

The crystalline structures of the films were investigated with Rigaku D/max 2500 VB+ XRD using Cu Kα radiation. The $\theta - 2\theta$ scans range is between 10° and 80° with a step size of 0.01°. From the broadening of the diffraction peaks, the crystallite size was estimated using the Scherrer formula [15]. The cross-sectional morphology of the TiO_2 thin films was observed with Philips Sirion 200 field emission SEM. The samples were covered with gold for SEM operation. The thickness of the films was measured by SEM and Alpha-Step IQ type profiler. Optical transmittance spectra of the films were investigated at room temperature with TU-1800 type UV–vis spectrophotometer. From the transmittance spectra, the optical constants of the films were calculated using the Swanepoel method [16].

3. Results and discussion

3.1. X-ray diffraction measurements

Fig. 1 shows the XRD spectra of TiO_2 films annealed at different temperatures. 'A' means the anatase phase, 'R' is the rutile phase. The average crystallite size of the TiO_2 thin films is estimated by the Scherrer's equation [15] as follows:

$$D_{hkl} = \frac{0.89\lambda}{\beta \cos\theta} \qquad (1)$$

where D_{hkl} denotes the average crystallite size of the TiO_2 thin films, $\lambda = 0.15405$ nm is the X-ray wavelength of Cu Kα, β is the width of the peak measured at half maximum intensity (FWHM) and θ is the Bragg's angle of the peak. The anatase crystallite size is calculated for the films annealed at temperatures lower than 900 °C, while the rutile crystallite size is calculated for the films annealed at 900 °C. The results are given in Table 1. The crystallite size of the films increases with the annealing temperature. The crystallite size of the films annealed at 900 °C is nearly twice that of the as-deposited films. The broad scattering peak occurring at 22° is from the substrate. As shown in Fig. 1, all the films are mixtures of anatase and rutile crystalline phases. When the annealing temperature is lower than 900 °C, the anatase is the main phase and exhibit a preferential orientation along the (1 0 1) plane. Anatase (1 0 1) peak shows a slight increase in its intensity with increasing annealing temperature. The intensity of rutile (1 1 0) peak shows an insignificant variation. That means the weight fraction of the anatase phase increases, while that of the rutile does not change significantly. It may arise from the phase transition from the amorphous to the anatase [17,18]. After the films are annealed at 900 °C, the intensity of rutile (1 1 0) peak increases significantly, while the anatase (1 0 1) peak becomes weak. That indicates the rutile phase is the dominating phase, and the anatase phase does not transform to rutile phase completely at 900 °C. The transition temperature of the anatase to rutile is about 900 °C, which is higher than 500 °C reported by Hunsche et al. [14]. Moreover, the mixed anatase/rutile structures can combine the effects of the higher transparency and surface area of anatase with the lower band gap of rutile. Nakaruk et al. have obtained the structures with mixed anatase and rutile phases, but also pure rutile phase at annealing temperatures of 900 °C [17]. In this paper, the mixed anatase/rutile phases still exist at annealing temperatures of 900 °C. This is a good result. It may arise from the different microstructure. It is worth noticing that the as-deposited TiO_2 films on the unheated substrates with mixed anatase and rutile phases were observed firstly for the sputtering method. Lrbl et al. thought that the oxygen particles impinging on the substrate promoted the nucleation of rutile [18]. In our experiment, the low sputtering pressure (0.7 Pa) and high oxygen ratio (10%) ensure the oxygen particles can hit the substrate with appreciable energy. According to Ref. [18], this could favor the nucleation of the rutile. Thereby, the rutile crystallite size is small. Besides, the deposition temperature can also influence the growth of the competing phases of rutile and anatase. In our experiment, the films were deposited at room temperature. Between about 25 °C and about 600 °C the anatase is a fast-growing phase whereas the rutile is growing very slowly [14]. Thus a mixed anatase/rutile structure is formed in the films.

3.2. Cross-sectional morphologies observed by SEM

SEM micrographs of the films annealed at different temperatures are shown in Fig. 2. It is observed that the as-deposited films exhibit a columnar structure. When the annealing temperature is below 900 °C, the columns grow thick and the film compactness increases with increasing the annealing temperature. This is because the incorporated atoms can move and adjust their positions in the titania network by a thermal diffusion process. After the films are annealed at 900 °C, the columnar structure disappears and some pores appear in the films. The density of rutile is 4.26 g/cm^3, whereas the anatase has a density of only 3.84 g/cm^3 [11]. From XRD, it is known that rutile phase becomes the main phase in the films annealed at 900 °C. Thus the imperfect densification led to the appearance of pores. It is worth noticing that anatase is the

Table 1
The crystallite size, refractive index (550 nm), extinction coefficient (550 nm), porosity and optical band gap of the TiO_2 films as-deposited and annealed.

Annealing temperature (°C)	Crystallite size (nm)		Refractive index at 550 nm	Extinction coefficient at 550 nm	Porosity (%)	Optical band gap (eV)
	Anatase	Rutile				
As-deposited	56	–	2.36	1×10^{-3}	14.5	3.32
300	64	–	2.42	8×10^{-4}	9.2	3.22
500	66	–	2.44	4×10^{-3}	7.4	3.22
700	84	–	2.47	4×10^{-3}	4.6	3.01
900	–	119	2.54	3×10^{-2}	14.1	2.57

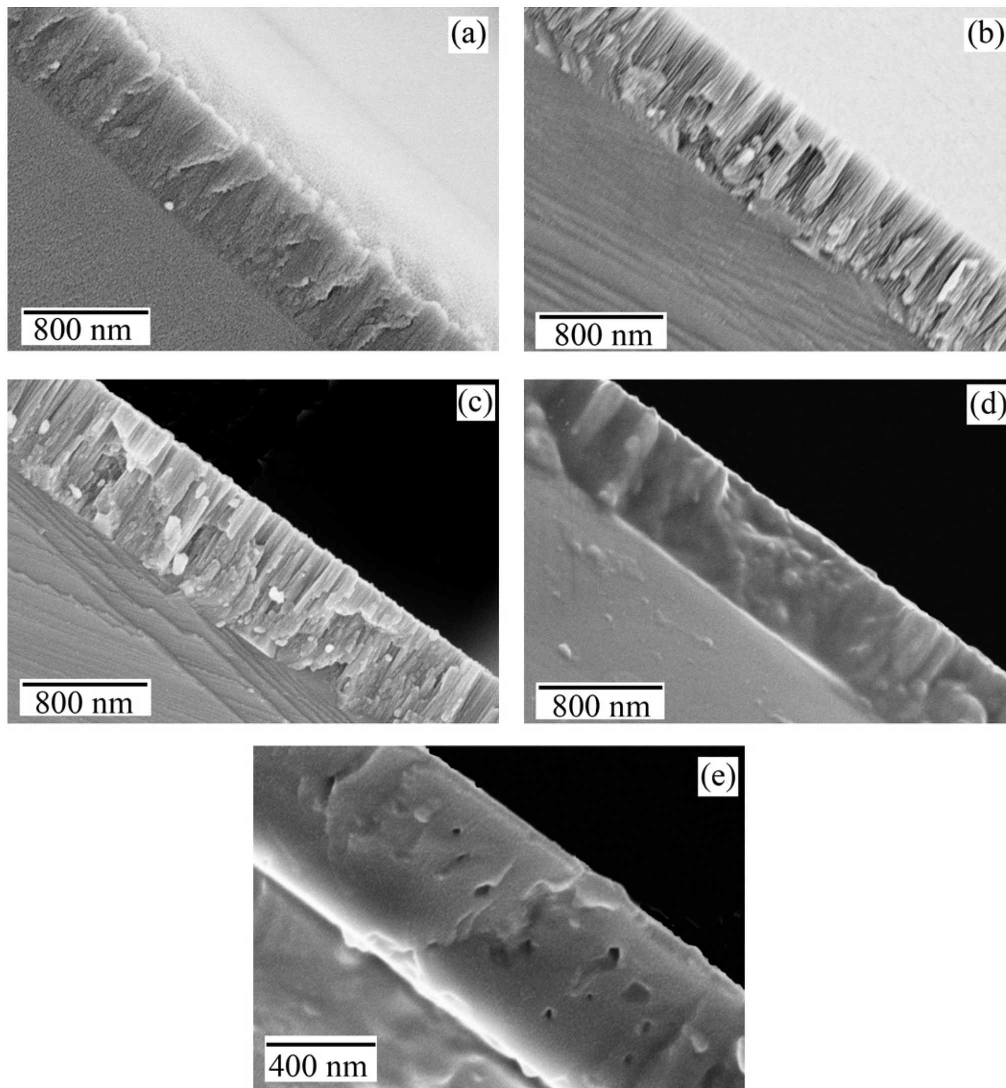

Fig. 2. SEM micrographs of the TiO_2 films annealed at different temperatures: (a) as-deposited; (b) 300 °C; (c) 500 °C; (d) 700 °C; (e) 900 °C.

main phase when the columnar structure exists in the films, and the rutile phase becomes the main phase when the annealing destroys the columnar structure. This indicates that the columnar structure restricts the transition of the anatase to rutile. This is because of the rutile nucleation at the boundary of two anatase particles during their annealing and a further migration towards the exterior of the new larger particle. This mechanism was observed firstly in the annealing of the anatase powders [19]. It can explain the difference between Nakaruk's results [17] and ours. Moreover, it can be derived from the mechanism that the crystallite size of the formed rutile films should be about twice that of the starting anatse films. The strong evidence can be found in the XRD results that the crystallite size of the films annealed at 900 °C is nearly twice that of the as-deposited films. It is worth noticing that the mechanism in thin films has not been reported before. As a result, the transition temperature is increased, which is consistent with the XRD results.

3.3. Transmittance spectra of TiO_2 thin films

Fig. 3 shows the transmittance spectra in UV–vis region of the quartz glass substrate and TiO_2 thin film samples annealed at different temperatures. The average transmittance of the as-deposited sample is 75%. When the annealing temperature is lower than 900 °C, the average transmittance is 76, 73 and 72% for the sam-

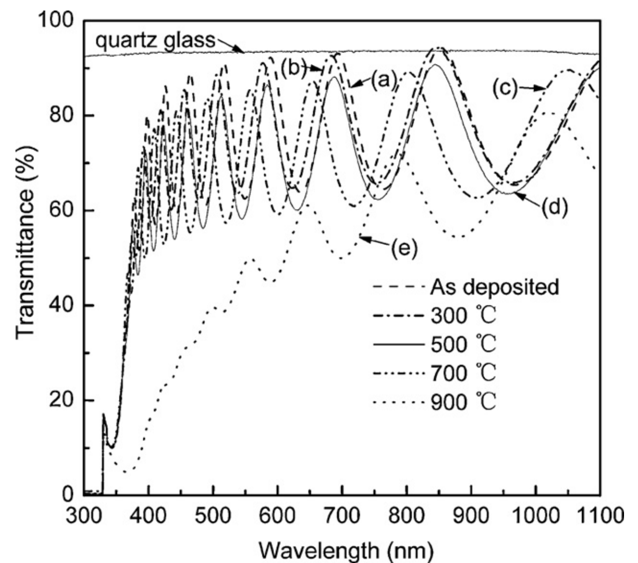

Fig. 3. Transmittance spectra of the TiO_2 films annealed at different temperatures: (a) as-deposited; (b) 300 °C; (c) 500 °C; (d) 700 °C; (e) 900 °C.

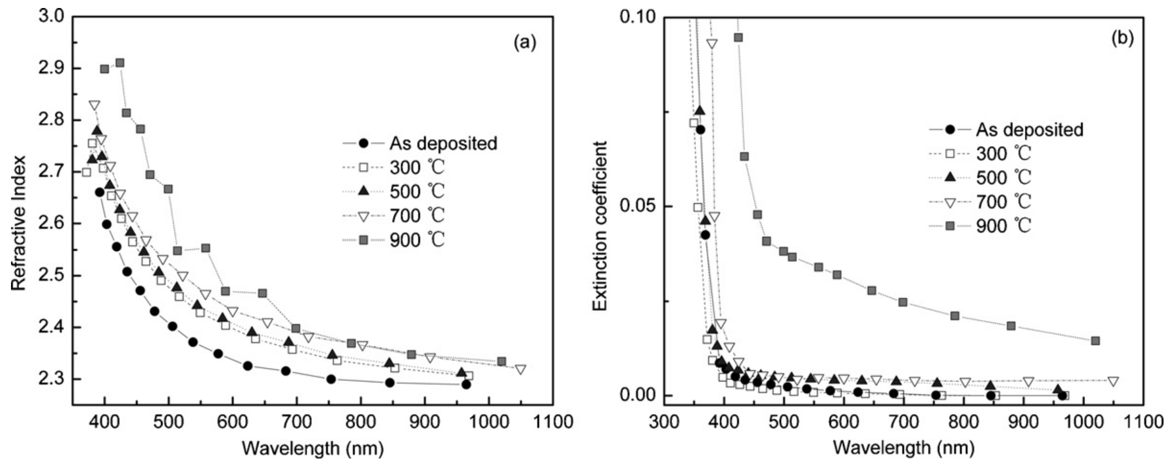

Fig. 4. Variation of refractive index and extinction coefficient for TiO_2 films: (a) refractive index; (b) extinction coefficient.

ples annealed at 300, 500 and 700 °C, respectively; an obvious absorption edge is observed around 380 nm. The transmittance improvement for the films annealed at 300 °C is due to the reduction of the unsaturated bonds [3]. The transmittance decreases with increasing the annealing temperature is due to the increase of scattering loss owing to crystallization. When the annealing temperature is up to 900 °C, the transmittance of the films decreases sharply and the absorption edge is around 480 nm. That is due to the absorption caused by the rutile phase.

3.4. Optical constants of TiO_2 films

According to the developed Swanepoel method [16], the refractive index and extinction coefficient of TiO_2 films were calculated. The refractive index n_f, in the spectral region of medium and weak absorption, can be calculated by the expression:

$$n_f = \sqrt{N + \sqrt{(N^2 - n_s^2)}} \tag{2}$$

where

$$N = 2n_s \frac{T_M - T_m}{T_M T_m} + \frac{n_s^2 + 1}{2} \tag{3}$$

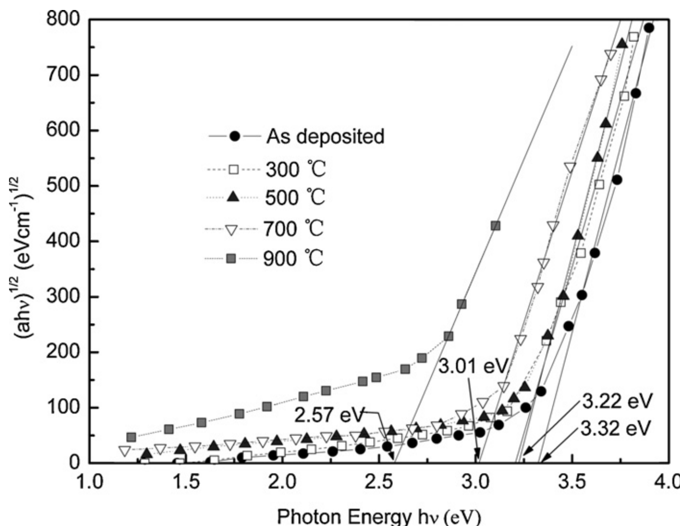

Fig. 5. Optical band gap for the TiO_2 films.

Here T_M and T_m are the transmission maximum and the corresponding minimum at a certain wavelength λ. The refractive index of the substrate n_s was derived by independently measuring the transmittance of the substrate T_s:

$$n_s = \frac{1}{T_s} + \left(\frac{1}{T_s} - 1\right)^{1/2} \tag{4}$$

The extinction coefficient k can be obtained from the expression:

$$k = -\frac{\lambda}{4\pi d} \ln \chi_\alpha \tag{5}$$

where the absorbance χ_α can be calculated from the interference-free transmission curves [16]. The film thickness d is about 700 nm, which is obtained from the SEM and profiler. The refractive index of the substrate is about 1.52 (at 550 nm).

The variation of the refractive index and extinction coefficient for TiO_2 films is shown in Fig. 4. The porosity of the films can be estimated by using the following expression [20]:

$$P = 1 - \frac{n_f^2 - 1}{n^2 - 1} \tag{6}$$

where n is the refractive index of bulk TiO_2. The values are 2.52 and 2.71 (at 550 nm) for the anatase and rutile bulk [20,21]. The refractive index at 550 nm and the porosity for the films as-deposited and annealed are given in Table 1. The refractive index of the as-deposited films is larger than those reported in other studies [11,13,20], being attributed to the higher packing density of the films [22]. When the annealing temperature is lower than 900 °C, the refractive index increases with the increase of the annealing temperature while the porosity decreases. The porosity increases after the films are annealed at 900 °C due to the appearance of pores in the films. The increase of refractive index arises from the denser rutile phase.

From Fig. 4b, it is found that the extinction coefficient decreases slightly for the films annealed at 300 °C, while the extinction coefficient increases for the films annealed at 500 and 700 °C. This is because unsaturated bonds are removed after the films are annealed at 300 °C [3], while the light scattering owing to crystallization is enhanced after the films are annealed at 500 and 700 °C. For the films annealed at 900 °C, there is a remarkable increase of the extinction coefficient because the anatase phase transforms to the rutile. Comparatively, the films annealed at 300 °C has higher refractive index and higher transparency over a wide spectral range, which means the film annealed at 300 °C has the best optical properties for the AR coatings.

The optical band gap E_g of the films is estimated by using the relation [16]:

$$(\alpha h\nu)^{1/2} = A(h\nu - E_g) \quad (7)$$

where $h\nu$ is the photon energy, E_g is the optical band gap and A is constant which does not depend on photon energy. The optical band gap of film is determined from the extrapolation of the linear plots of $(\alpha h\nu)^{1/2}$ versus $h\nu$ at $\alpha = 0$. α is absorption coefficient. The optical band gap for the films is shown in Fig. 5. The values of band gap for the films as-deposited and annealed are given in Table 1. It is found that the band gap of the films decreases with increasing annealing temperature. Moreover, the optical band gap is smaller than that reported in Refs. [8,20]. This behavior is probably due to the rutile phase in the films, which has a lower band gap [23].

4. Conclusions

The films prepared on unheated substrates by DC reactive magnetron sputtering, are mixtures of anatase and rutile phases, which is observed for the first time. The films possess a column-like texture, and the columnar structure restricts the transition of anatase to rutile. When the annealing temperature is lower than 900 °C, the anatase phase is the dominant crystalline phase, the weight fraction of the rutile phase does not increase significantly during annealing process. As the annealing temperature rises to 900 °C, the rutile phase becomes the dominant crystalline phase, and the columnar structure disappears. The refractive index of the films increases from 2.36 to 2.54 (at 550 nm) with the annealing temperature, while their extinction coefficients increase from 8×10^{-4} to 0.03 (at 550 nm). The optical band gap of the films decreases from 3.32 eV to 2.57 eV as the annealing temperature increases.

Acknowledgement

This work is supported by the Hunan Province Key Project of Science and Technology (Project no. 08FJ1002).

References

[1] B.S. Richards, J.E. Cotter, C.B. Honsberg, Appl. Phys. Lett. 80 (2002) 1123–1125.
[2] M. Zribi, M. Kanzari, B. Rezig, Thin Solid Films 516 (2008) 1476–1479.
[3] W.H. Wang, S. Chao, Opt. Lett. 23 (1998) 1417–1419.
[4] G. Shukla, P.K. Mishra, A. Khare, J. Alloys Compd. 489 (2010) 246–251.
[5] H. Ogawa, T. Higuchi, A. Nakamura, S. Tokita, D. Miyazaki, T. Hattori, T. Tsukamoto, J. Alloys Compd. 449 (2008) 375–378.
[6] R. Tang, W. Zhang, Y. Li, J. Alloys Compd. 496 (2010) 380–384.
[7] H.J. Frenck, W. Kulisch, M. Kuhr, R. Kassing, Thin Solid Films 201 (1991) 327–335.
[8] D. Yoo, I. Kim, S. Kim, C.H. Hahn, C. Lee, S. Cho, Appl. Surf. Sci. 253 (2007) 3888–3892.
[9] G. Mincuzzi, L. Vesce, A. Reale, A.D. Carlo, T.M. Brown, Appl. Phys. Lett. 95 (2009) 103312.
[10] H. Rath, P. Dash, T. Som, P.V. Satyam, U.P. Singh, P.K. Kulriya, D. Kanjilal, D.K. Avasthi, N.C. Mishra, J. Appl. Phys. 105 (2009) 074311–074315.
[11] S.B. Amor, L. Guedri, G. Baud, M. Jacquet, M. Ghedira, Mater. Chem. Phys. 77 (2002) 903–911.
[12] G. Tian, L. Dong, C. Wei, J. Huang, H. He, J. Shao, Opt. Mater. 28 (2006) 1058–1063.
[13] Y.Q. Hou, D.M. Zhuang, G. Zhang, M. Zhao, M.S. Wu, Appl. Surf. Sci. 218 (2003) 97–105.
[14] B. Hunsche, M. Verghl, A. Ritz, Thin Solid Films 502 (2006) 188–192.
[15] M.C. Wang, H.J. Lin, T.S. Yang, J. Alloys Compd. 473 (2009) 394–400.
[16] E. Marquez, J. Ramirez-Malo, P. Villares, R. Jimenez-Garay, P.J.S. Ewen, A.E. Owen, J. Phys. D: Appl. Phys. 25 (1992) 535–541.
[17] A. Nakaruk, C.Y. Lin, D.S. Perera, C.C. Sorrell, J. Sol–Gel Sci. Technol. 55 (2010) 328–334.
[18] P. Löbl, M. Huppertz, D. Mergel, Thin Solid Films 251 (1994) 72–79.
[19] J.M.G. Amores, V.S. Escribano, G. Busca, J. Mater. Chem. 5 (1995) 1245–1249.
[20] M.M. Hasan, A.S.M.A. Haseeb, R. Saidur, H.H. Masjuki, M. Hamdi, Opt. Mater. 32 (2010) 690–695.
[21] G. Hass, Vacuum 2 (1952) 331–345.
[22] D Mardare, Rom. J. Phys. 45 (2000) 571–577.
[23] D. Mardare, G.I. Rusu, Mater. Lett. 56 (2002) 210–214.